

Technological Educational Institute of Crete

School of Engineering

Department of Informatics Engineering

# Gene expression and gene regulatory network analysis with statistical methods and machine learning algorithms

*Student*

Fotini Droumalia

*Supervisor*

Lefteris Koumakis

Heraklion **Month**, 2022

## **Abstract**

# Table of Contents

Abstract	1
List of Tables	4
List of Figures	4
Introduction	5
Pathway Analysis Tools	6
TAPPA	6
SPIA	6
TopologyGSA	8
PARADIGM	10
GGEA	12
HotNet	13
PRS	16
DEGraph	18
TEAK	21
PATHiWAYS	22
DEAP	23
GraphiteWeb	24
PATHOME	25
SubSPIA	26
MinePath	26
HiPathia	28
Materials and Methods	31
Datasets and processing	31
Computing the score	31
Subpathway ranking	32
Results	34

Predictive performance/ Data validation	34
Tools comparison	35
Discussion	37
Conclusions	39
References	40

## List of Tables

<b>Table 1.</b> Pathway's scoring formula of Pathways Analysis tools .....	29
<b>Table 2.</b> Predictive performance of each tool .....	34

## List of Figures

<b>Figure 1.</b> Pseudocode for the combinatorial model's algorithm.....	14
<b>Figure 2.</b> Nonhomogeneous subgraph discovery algorithm .....	19
<b>Figure 3.</b> Predictive Performance of each tool based on the method.....	35

## Introduction

Pathway Analysis (PA), also called functional enrichment analysis, is becoming more and more important in Omics research, which concerns biological branches that end with the suffix –omics [1]. Pathway Analysis methodologies combine knowledge from gene expression analysis and molecular pathway networks to discover strongly impacted pathways in a given condition and better understand the biological significance of differentially expressed genes and proteins.

The term Pathway refers to the graphical representation of molecular interaction, reaction, and relationship networks. The graph consists of nodes, which correspond to genes, proteins, and/or molecules, and directed edges, which represent relationships and interactions between the nodes. The states of each gene are either on or off, indicating whether the gene is expressed or not expressed respectively. The types of interactions between the nodes vary. Activation, inhibition, and catalysis are some examples of different sorts of interactions between nodes.

Pathway analysis techniques discover the pathways that are strongly impacted in a specific circumstance by combining available pathway databases with gene expression data [2]. KEGG, Reactome, and BioCarta are some of the sources that include thorough information about pathways. KEGG is a repository of hand-drawn pathway maps that provide information about genomes, biological pathways, diseases, pharmaceuticals, and chemical compounds [3], [4], while BioCarta's interactive online services give the means to see how genes communicate in dynamic graphical models [5]. Reactome database's mission is to provide user-friendly bioinformatics tools for visualizing, interpreting, and analyzing pathway data in support of fundamental and medical trials, genomic analysis, modeling, systems biology, and education [6].

We can distinguish two main approaches to pathway analysis: the first one takes into consideration only the expression levels of the genes of a pathway, while the second one takes advantage of the pathway topology as well, known as topology-based [7].

The aim of this study is to identify similarities and differences between distinct pathway activity analysis tools, which are based on statistical and machine learning methods.

## Pathway Analysis Tools

### TAPPA

TAPPA is a java-based tool that was introduced in [8] and uses pathway topological measurements to identify phenotype-associated genomic circuits. This is accomplished by calculating a Pathway Connectivity Index (PCI) for each pathway and then assessing its relationship to phenotypic variance.

$$PCI = \sum_{i=1}^N \sum_{j=1}^N sgn(x_{is} + x_{js}) * |x_{is}|^{0.5} * \alpha_{ij} * |x_{js}|^{0.5}$$

In the formula above,  $x_{is}$  stands for the standardized log expression measurement for gene  $i$  and sample  $s$ .  $N$  represents the total of genes, and  $sgn(x_{is} + x_{js})$  denotes the overall expression status (up- or down-regulation) of the gene pair. Given that a pathway can be visualized as a graph  $G(V, E)$ , the adjacency matrix is defined as  $A = (\alpha_{ij})$ , such that  $\alpha_{ij} = 1$  if  $i = j$  or  $(g_i, g_j) \in E$ , otherwise  $\alpha_{ij} = 0$ .

Subsequently, each PCI value is divided by the number of genes in the respective pathway in order to normalize the PCIs.

The TAPPA tool was developed using JAVA and can handle both binary and numerical attributes. In the case of the binary traits, the Mann–Whitney test is used to assess the significance of the relationship between network PCI and phenotype, while the Spearman correlation is used for continuous attributes. In addition, a permutation test is used to assess the false discovery rate (FDR).

Subsequently, using different zoom ratios, the pathway is visualized and the genes that are strongly related to the phenotype are identified. Eventually, the relationship between the phenotypes of the sub-modules in a pathway is studied and determines the biological significance of the genes involved.

### SPIA

Signaling Pathway Impact Analysis, also known as SPIA, uses data collected from the classical enrichment analysis and combines them with data that evaluate the perturbation of a certain pathway under a specific circumstance. The following methodology is described in [9].

Impact Analysis considers the overrepresentation of DE genes in a particular pathway and the anomalous alteration of that pathway, as determined by propagating observed expression changes across the pathway topology. These features correspond to two separate probabilities,  $P_{NDE}$  and  $P_{PERT}$ .

The  $P_{NDE} = P(X \geq N_{de}|H_0)$  probability represents the importance of a pathway  $P_i$ , based on an overrepresentation study of the number of DE genes ( $N_{DE}$ ) found on the pathway.

$P_{PERT}$  probability results from the degree of perturbation in each pathway, which is calculated using the following gene perturbation function:

$$PF(g_i) = \Delta E(g_i) + \sum_{j=1}^n \beta_{ij} \cdot \frac{PF(g_j)}{N_{ds}(g_j)}$$

The above formula takes into consideration the type of relationship between two genes and is represented by the term  $\beta_{ij}$ . If the value of  $\beta$  equals to +1, then the type of interaction is activation, while -1 corresponds to inhibition and repression.

The net perturbation accumulation at the gene level,  $Acc_g$ , is then calculated as the difference between a gene's perturbation factor PF and its signed adjusted expression change or observed log fold-change, when comparing two circumstances.

$$Acc(g_i) = PF(g_i) - \Delta E(g_i)$$

Subsequently, the total net accumulated perturbation of a pathway is calculated as the sum of the net perturbation accumulation of each gene.

$$t_A = \sum_i Acc(g_i)$$

The possibility of seeing a total accumulated perturbation of the pathway,  $T_A$ , greater than  $t_A$ , is represented by the  $P_{PERT}$  probability:

$$P_{PERT} = P(T_A \geq t_A|H_0)$$

Eventually,  $P_{NDE}$  and  $P_{PERT}$  are integrated into a global probability value,  $P_G$ . Through this probability value the pathways are ranked, and the hypothesis is tested to see if the pathway is significantly disrupted in the study condition.

$$P_G = c_i - c_i \cdot \ln(c_i), \quad c_i = P_{NDE}(i) \cdot P_{PERT}(i)$$



$P_G$  can also set the level of type I error. It is recommended to use the common FDR approach to keep the false discovery rate (FDR) of the pathway analysis at 5%.

## TopologyGSA

This method evaluates the differential expression of a pathway using graphical models as demonstrated in [10]. Then it illustrates the components of the pathway that are implicated in the deregulation. Below is a detailed description of the technique.

In this project, KEGG maps are employed, since they provide a good ratio between map accuracy and simplicity. Initially, the paths obtained from the KEGG repository are transformed into a graphical model. This is accomplished by using the following basic steps: i) simple directed edges include inhibition, phosphorylation (+p), and dephosphorylation (-p); ii) BioCarta network provides extensive information that can be used to direct undirected edges and iii) when it comes to complexes (nodes consisted of several gene products), the first principal component is defined as the complex's expression. The data of the same pathway are represented in distinct experimental states as implementations of undirected graphical Gaussian models with the same undirected graph  $G$ . For instance, in the case of two scenarios, we employ the Gaussian models

$$M_1(G) = \{Y \sim N_p(\mu_1, \Sigma_1), \Sigma_1^{-1} \in S^+(G)\},$$

$$M_2(G) = \{Y \sim N_p(\mu_2, \Sigma_2), \Sigma_2^{-1} \in S^+(G)\}.$$

In this case,  $p$  refers to the number of genes (nodes of the graph), while  $S^+(G)$  represents the array of symmetric positive definite matrices with null components indicating the missing connections of  $G$ .

The estimated covariance matrices are calculated by using a technique known as the Iterative Proportional Scaling Technique (IPS) for graph analysis, which ensures that the estimated matrices are positive definite and that their inverse has null elements correlating to the graph's missing edges. The sample covariance matrices can be generated, either from the chip covariance matrices by removing elements referring to all the pairs of genes in the pathway, or by determining the expression levels of the genes on the pathway and measuring the sample covariances.

Then, to compare the gene sets among two experimental conditions, the null hypothesis testing method is employed. The strength of the connections that define a pathway can

vary under different situations, causing changes in the pathway's expression. The equivalence of two means is the corresponding hypothesis. The evaluation is determined by whether the models' covariances, which are often unknown, are homogeneous. As a result, the choice of the homogeneity hypothesis has an impact on the analysis of the means.

Eventually, the strength of the gene relationships in two experimental conditions is put to the test to see if they are equal. This is easily accomplished in the context of graphical Gaussian models by comparing the two concentration matrices (opposite of the covariance matrices), which include all the details about the underlying structure. As a result, the focus is on putting the hypothesis  $\Sigma_1^{-1} = \Sigma_2^{-1}$  to the test.

The methods for comparing covariance matrices are then applied to the specific instance of graphical Gaussian models in the following methodology. Assume that  $\gamma_1 = (\gamma_1^j)$ ,  $j = 1, \dots, n_1$  observations from  $N_p(0, \Sigma_1)$ , and  $\gamma_2 = (\gamma_2^j)$ ,  $j = 1, \dots, n_2$  observations from  $N_p(0, \Sigma_2)$ , with  $\Sigma_1^{-1} = K_1 \in S^+(G)$  and  $\Sigma_2^{-1} = K_2 \in S^+(G)$  without losing generality. The hypothesis to be tested is  $H_0: K_1 = K_2$  against  $H_1: K_1 \neq K_2$ . When the value of  $W_i$  is determined using the function  $W_i = \sum_{j=1}^{n_i} (\gamma_i^j)(\gamma_i^j)^T$ ,  $i = 1, 2$ , the likelihood function,  $L(K_1, K_2)$ , yields as follows:

$$L(K_1, K_2) = \prod_{i=1}^2 (2\pi)^{-\frac{n_i p}{2}} (\det \det K_i)^{\frac{n_i}{2}} e^{-\frac{1}{2} \text{tr}(K_i W_i)}$$

Starting with the pooled covariance matrix  $S = (n_1 + n_2 - 2)^{-1} \cdot \{(n_1 - 1) \cdot S_1 + (n_2 - 1) \cdot S_2\}$  and the null hypothesis, the technique calculates the estimate,  $\hat{\Sigma}$ , of the common covariance matrix. On the contrary, under the alternative hypothesis, the sample covariance matrices,  $S_1 = (n_1 - 1)^{-1} \cdot W_1$  and  $S_2 = (n_2 - 1)^{-1} \cdot W_2$ , are used, so that the values of  $\hat{\Sigma}_1$  and  $\hat{\Sigma}_2$  are calculated.

After making several assumptions, the likelihood ratio test,  $\Lambda$ , is computed using the following formula:

$$\Lambda = \frac{L_{H_0}(\hat{K}_1, \hat{K}_2)}{L_{H_1}(\hat{K}_1, \hat{K}_2)} = \frac{L_{H_0}(\hat{K})}{L_{H_1}(\hat{K})}$$

It is also true that by letting  $W = W_1 + W_2$  and taking advantage of the fact that  $tr(\hat{K}_i W_i) = n_i tr(\hat{K}_i \hat{K}_i^{-1}) = n_i p$  and  $tr(\hat{K} W) = (n_1 + n_2) tr(\hat{K} \hat{K}^{-1}) = (n_1 + n_2) p$ , the following two formulas emerge.

$$\Lambda = \prod_{i=1}^2 \left( \frac{\det \hat{K}}{\det \hat{K}_i} \right)^{\frac{n_i}{2}}$$

$$-2 \log \Lambda = \sum_{i=1}^2 n_i \log \left( \frac{\det \hat{K}_i}{\det \hat{K}} \right)$$

If indeed the null hypothesis is false, the graphical methodology enables us to evaluate the causes of differences between the two concentration matrices. In particular, if the graph is decomposable, it is feasible to break it down into its maximal complete sub-graphs (cliques) and perform the preceding test for each clique. Following the standard procedures, the equivalence of the covariance matrices on cliques can be evaluated. However, if the graph is not divisible, more edges can be introduced to create a new triangulated and thus decomposable graph. The graph's cliques can then be used to conduct the test.

Eventually, the pathway's differential expression is examined. The differential expression of the pathway, if the null hypothesis is not rejected, is evaluated by hypothesis

$$H_0: \mu_1 = \mu_2 \text{ subject to } \Sigma_1 = \Sigma_2.$$

Exact approaches, such as multivariate analysis of variance, can be used to carry out this test. If the null hypothesis of homogeneity is rejected, the hypothesis that must be tested is

$$H_0: \mu_1 = \mu_2 \text{ subject to } \Sigma_1 \neq \Sigma_2.$$

In a two-sample scenario with unequal covariance matrices, this is the standard test for equality of means, also known as the Behrens-Fisher problem.

## PARADIGM

PARADIGM stands for Pathway Recognition Algorithm using Data Integration on Genomic Models and aims to infer the activity of genetic pathways from integrated patient data. The methodology is outlined in [11] and is summarized below.

The implementation starts by creating a separate probabilistic model for each pathway. A factor graph was created using a pathway diagram that included both concealed and observable states. Also, we employ variables to characterize the states of entities in a cell to illustrate a biological pathway with a factor graph.

The factor graph uses a random variable  $X = x_1, x_2, \dots, x_n$  for each entity and a set of  $m$  non-negative functions, or factors, to restrict the entities' ability to take on biologically meaningful values as functions of one another to represent the status of a cell. A probability distribution over a subset of entities  $X_j \subset X$  is defined by the  $j$ -th factor  $\phi_j$ . The joint probability distribution over all the entities is encoded in the whole graph of entities and factors as follows:

$$P(X) = \frac{1}{Z} \prod_{j=1}^m \phi_j(X_j)$$

Each entity can be active, nominal, or deactivated in relation to a control level, and these states are encoded as 1, 0 or -1 correspondingly.

To make factor building easier, we turn the pathway into a directed graph, with each edge annotated with a positive or negative influence. In the directed graph, every interaction in the pathway is turned to a single edge. Then, a list of factors is created to define the factor graph using this directed graph. Eventually, we complete the integration of pathway and multi-dimensional functional genomics data by adding observation variables and factors to the factor graph.

Subsequently, we want to know if a particular hidden entity  $x_i$  is likely to be in state  $\alpha$  based on patient data.

$$P(x_i = \alpha | \Phi) = \frac{1}{Z} \prod_{j=1}^m \sum_{S \sqsubset_{A_i(\alpha)} X_j} \phi_j(S)$$

Similarly, the likelihood that  $x_i$  is in state  $\alpha$ , based on all the patient's observations, is:

$$P(x_i = \alpha, D | \Phi) = \frac{1}{Z} \prod_{j=1}^m \sum_{S \sqsubset_{A_i(\alpha) \cup D} X_j} \phi_j(S)$$

The expectation-maximization (EM) technique is used to estimate the parameters of the observation factors. A factor graph for each patient is generated, the patient's data are applied, and EM runs until the likelihood changes by less than 0.1 percent for each

pathway. The factors learned from each pathway were averaged, and the final posterior estimates for each variable were calculated using these parameters.

Afterwards, a matrix of Integrated Pathway Activities (IPA) is generated for each variable with an ‘active’ molecular type after inference. A log-likelihood ratio that describes the level to which a patient's data boosts our opinion that entity  $i$ 's activity is up or down is calculated based on the following formula.

$$L(i, \alpha) = \log \left( \frac{P(D, x_i = \alpha | \Phi)}{P(D, x_i \neq \alpha | \Phi)} \right) - \log \left( \frac{P(x_i = \alpha | \Phi)}{P(x_i \neq \alpha | \Phi)} \right) = \log \left( \frac{P(D, x_i = \alpha, \Phi)}{P(D, x_i \neq \alpha, \Phi)} \right)$$

Based on the log-likelihood ratio, a single IPA for gene  $i$  is computed as follows:

$$IPA(i) = \begin{cases} L(i, 1), & L(i, 1) > L(i, -1) \text{ and } L(i, 1) > L(i, 0) \\ -L(i, -1), & L(i, -1) > L(i, 1) \text{ and } L(i, -1) > L(i, 0) \\ 0, & \text{otherwise} \end{cases}$$

The IPA score is a signed equivalent of the log-likelihood ratio,  $L$ . It is set to  $L$  if the gene is more likely to be activated. If the gene is more likely to be inhibited, the IPA is set to  $-L$ ; otherwise, it is set to 0.

Two alternative permutations of the data are used to measure the significance of IPA scores. A permuted data sample is constructed for the 'within' permutation by selecting a random tuple of data first from a random real sample, and then from a random gene within the same network, until tuples have been selected for each gene in the pathway, while the technique for the 'any' permutation is much like the 'within' permutation method, except the random gene selection stage could pick a gene from anywhere in the genome. In both cases, 1000 permuted samples are constructed, and perturbation scores are calculated for each permuted sample. To evaluate the significance of real samples, the distribution of perturbation scores from permuted samples is employed as a null distribution.

## GGEA

Gene Graph Enrichment Analysis (GGEA), as stated in [12], is a method that uses previous information acquired from directed gene regulation networks to find consistently and coherently enriched gene sets.

The method on which GGEA is based consists of three critical stages. Initially, to create an induced subnetwork, the gene set is first mapped into the fundamental regulatory

network. This is the part of the network that is impacted, which is made up of edges that involve members of the gene set. Next, each edge of the induced network is evaluated for consistency with the expression data, i.e. the signals of two interaction partners' expression changes are compared to the regulatory type (activation/inhibition) of the link connecting both genes. Finally, using a permutation process, the edge consistencies are aggregated over the induced network, normalized, and significance evaluated.

Consistency is calculated using the following formula:

$$C(t) = \text{cons}(de_o, f_t(de_i))$$

The raw GGEA consistency score  $S$  is induced by summing the consistency of all gene regulatory network (GRN) transitions and then normalized by the number of transitions, to compensate for the GRN's size.

$$S := \sum_{t \in T_u} C(t)$$

$$\bar{S} := \frac{S}{|T_u|}$$

Eventually, for each gene set we estimate the consistency P-value and rank the gene sets based on the adjusted P-values. Gene sets that are significantly and persistently enriched fall below the predefined significance level.

## HotNet

HotNet is another approach for detecting significantly altered subnetworks in a large gene interaction network, that was initially designed for cancer mutation data [13]. The method for identifying cancer pathways that have been significantly mutated is presented below and is based on [14].

First, the model that will be used for the interpretation of the data is defined. Graph  $G = (V, E)$  is used to model the interaction network, while  $T \subseteq V$  corresponds to a subgroup of the genes that were tested. Each  $g$  gene is classified as either mutant or normal. The notation  $M_i$  is used to describe a subset of mutant genes in group  $T$ , while  $S_j$  denotes the samples under which the gene  $g_j \in T$  has been altered, and  $m$  indicates the total number of mutant genes detected across all samples. A linked subgraph of  $G$  is defined as the resultant pathway.

After that, the influence graph, that encodes the knowledge in the interaction network, is constructed. The importance of a subnetwork is determined by (i) the number of samples with mutations in the subnetwork's genes, and (ii) the linkages among genes in the subnetwork in the context of the overall network's topology. On the interaction network, a diffusion process is employed to create a strict level of influence across all network nodes. The procedure outlined by Qi et al. (2008) is used to calculate the effect of node  $s$  on all other nodes in the network, and therefore, the influence graph  $G_I = (T, E_I)$  with the collection of nodes belonging to the subset of tested genes is obtained. The weight of each edge  $w(g_j, g_k) = [i(g_k, g_j), i(g_j, g_k)]$  is also considered.

Then, to discover altered paths, a combinatorial model is developed. First, collections of nodes in the influence graph  $G_I$  that are (1) related by high-influence links and (2) relate to mutated genes in many samples, are selected. A threshold  $\delta$  is determined and, by deleting all edges with  $w(g_i, g_j) < \delta$  and all nodes belonging to genes in the sample data with no modifications, a reduced impact graph  $G_I(\delta)$  of  $G_I$  is constructed. Consequently, the size of the identified related subgraphs is determined by a threshold  $\delta$ , which is entirely reliant on the null hypothesis. The connected maximum coverage problem, which is an NP-hard problem, is analogous to discovering the linked subgraph of  $k$  genes that is mutated in the maximum number of samples. To make the algorithm run properly, a modified version of the combinatorial algorithm shown in [Figure 1](#) is used, in which for each pair of nodes  $(u, v)$ , all the shortest paths between  $u$  and  $v$  are evaluated, and the one that optimizes  $\frac{|P_v(u)|}{|l_v(u)|}$  is preserved.

**Figure 1.** Pseudocode for the combinatorial model's algorithm

---

*Combinatorial Algorithm*

---

**Input:** Influence graph  $G_I$  and parameters  $\delta$  and  $k$

**Output:** Connected subgraph  $C$  of  $G_I(\delta)$  with  $k$  vertices

1. Construct  $G_I(\delta)$  by removing from  $G_I$  all edges with weight  $< \delta$ ;
  2.  $C \leftarrow \emptyset$ ;
  3. **for** each node  $v \in V$  **do**
  4.    $C_v \leftarrow \{v\}$ ;
  5.   **for** each  $u \in V \setminus \{v\}$  **do**  $p_v(u) \leftarrow$  shortest path from  $v$  to  $u$  in  $G_I(\delta)$ ;
  6.   **while**  $|C_v| < k$  **do**
-

---

$//\ell_v(u) = \text{set of nodes in } p_v(u); P_v(u) =$   
 $\text{elements of } I \text{ covered by } \ell_v(u); P_{C_v} =$   
 $\text{elements covered by } C_v; P_C = \text{elements covered by } C$

7.  $u \leftarrow \arg \max_{u \in V \setminus C_v: |l_v(u) \cup C_v| \leq k} \left\{ \frac{|P_v(u) \setminus P_{C_v}|}{|l_v(u) \setminus C_v|} \right\};$
8.  $C_v \leftarrow \ell_v(u) \cup C_v;$
9. **if**  $|P_{C_v}| > |P_C|$  **then**  $C \leftarrow C_v$
10. **return**  $C;$

---

Subsequently, to detect mutated subnetworks, a computationally efficient enhanced influence model is generated. The Enhanced Influence Model is rooted in the idea of increasing the influence measure among genes by the number of mutations found in each of these genes, and then breaking the resulting enhanced influence graph into linked components.

$H$  refers to the enhanced influence graph. All genes  $g_j$  having at least one mutation in the data make up the set  $V_H$  of  $H$ 's vertices, while the improved influence

$$h(g_j, g_k) = w(g_j, g_k) \times \{|S_j|, |S_k|\}$$

determines the weight of the edge  $(g_j, g_k)$ . Then, to produce a graph  $H(\delta)$ , whose linked components represent the significant subnetworks, any edges with a weight less than a threshold  $\delta$  are eliminated.

Eventually, a statistical analysis is performed to determine the network's significance. There are two null hypothesis distributions considered:

- i.  $H_0^{sample}$  in which  $m = \sum_i |M_i|$  mutations are randomly distributed throughout the nodes correlating to the  $|T|$  tested genes
- ii.  $H_0^{gene}$  which is obtained by permuting the identities of the network's evaluated genes, using a random permutation  $\sigma$

A two-stage multi-hypothesis test is executed and the Family Wise Error Rate (FWER), that is the probability of making at least one Type I error in any of the tests, is used as the rigorous indicator of its significance level. The False Discovery Rate is a less conventional alternative to minimizing errors in multiple testing (FDR). It is denoted as  $FDR = E[V/R]$ , where  $V$  represents the number of Type I errors and  $R$  represents the



total amount of null hypotheses excluded. The two-stage test identifies several subnetworks in the data as statistically significant with low FDR values.

Using a similar approach to that used in the Combinatorial model, it is shown in this study how the number of hypotheses can be limited to merely  $K = |T|$  hypotheses. The first stage of evaluating each hypothesis with confidence level  $\alpha/K$  determines the smallest size  $s$ , such that the null hypothesis that the number of linked components of size  $\geq s$  detected in the graph  $H(d)$ ,  $r_s$ , may be rejected with confidence level  $\alpha$ . The test also includes a second criterion that ensures that the FDR is kept within a certain range.

A Monte-Carlo simulation ("permutation test") or analytical bounds can be used to calculate the null hypothesis distributions. Two properties of the Monte-Carlo simulation approach considerably minimize the cost of the estimations. The Monte Carlo simulation must be done on the graph  $G_I$ . The  $p$ -value of the distribution of the number of connected linked subgraphs/components of a particular size is used in the statistical test. As a result, it is essential to determine  $p$ -values that are a magnitude larger for this test, using vastly fewer simulation rounds.

Using analytical bounds, the null hypothesis can be approximated for a greater number of tested genes. For any node  $g_i$  in  $G_I$ , the maximum  $\delta$  is set such that the weight of less than  $\alpha M/|T|$  connected edges gratify  $s_{max}w(g_i, g_j) \geq \delta$ , for any given  $\alpha < 1$ .

## PRS

Pathway Regulation Score, or else PRS, is a method which distinguishes between essential processes in real-world biological datasets. The procedure that follows is a simplified version of the method as described in [15].

The data were first pre-processed using the Robust Multiarray Average (RMA) approach, and the DEG lists were produced using simple fold change and  $p$ -value calculations. The pathways retrieved by the KEGG database were represented in the form of a graph. Due to redundancies in KEGG pathways, fold-change values for a node may be assigned to a route several times, resulting in a skewed PRS calculation. Consequently, a new structure emerged, in which duplicated genes were unified into a single term with a unique ID.

In order to implement the PRS algorithm, the pathways were represented as networks, so that each pathway is characterized by a unique identity, definition name, and its corresponding nodes. Particularly, a pathway's nodes are described by the following attributes. *Node\_genes* correspond to a distinct function that maps to one or more transcripts and *Node\_value* (*NV*) represents a value based on expression data. *Node\_weight* (*NW*) concerns only the significant nodes and indicates their structural strength. The *Node\_Score* (*NS*) is calculated by combining the *NV* and *NW* values.

$$NS = \begin{cases} NV * NW & \text{if } NV > 1 \\ 0 & \text{if } NV \leq 1 \end{cases}$$

Subsequently, using the following formula the PRS is determined:

$$PRS(p_i) = \sum_{j=1}^{n_i} NS_j$$

Prior to rating the paths, a normalization step is performed to account for two crucial features.

- i. Pathway size: the bias caused by pathway size was reduced as seen in the following equation.

$$PRS(p_i) = \left( \sum_{j=1}^{n_i} NS_j \right) * \left( \frac{NDEGS_i}{NEGS_i} \right)$$

- ii. Pathway-specific PRS score null distributions that contribute to statistical bias: a nonparametric permutation approach is employed to determine the null distributions of raw PRS values acquired for each pathway.

$$nPRS_i = \frac{PRS_i - \text{mean}(pPRS_i)}{STD(pPRS_i)}$$

$$npPRS_{ij} = \frac{pPRS_{ij} - \text{mean}(pPRS_i)}{STD(pPRS_i)}$$

For pathway ranking, the normalized raw scores ( $nPRS_i$ ) were used.

To determine the significance, the PRS values were recalculated using the equation used to reduce the bias caused by the pathway size, after the fold-change values for the full gene list were permuted and mapped back onto pathways. To construct a null distribution of each raw score, this procedure was repeated 1000 times. Then, the normalized scores were compared, and the p-values were determined as shown below:

$$P(nPRS_i) = \frac{\sum_{j=1}^n I(npPRS_{ij} \geq nPRS_i)}{n}$$

Finally, a multiple test adjustment was implemented, and the FDR modified the  $P_{\text{final}}$  to account for type I errors.

## DEGraph

DEGraph is yet another pathway analysis tool that uses modern hypothesis testing approaches to predict whether a specific gene network is differentially expressed between two scenarios and is very useful in cancer research [16]. The step-by-step methodology is defined in [17].

First, a lower-dimension basis is constructed, after which the multivariate test of means is used. The testing question of whether two sets of random vectors of gene expression measures are expected to have emerged from equal-mean distributions, can be directly formulated, and solved using multivariate statistics.

A network of  $p$  genes is depicted as graph  $G = (V, E)$ , having  $|V| = p$  nodes and edge set  $E$ , while  $\delta$  refers to the mean shift, to wit, the vector of differences between the  $p$  genes' mean expression values among the two study populations. Afterwards, a lower-dimensional  $k \ll p$  space is constructed, retaining most of the low-energy functions  $E_G(\delta)$ . To accomplish this, the function with the least potential energy is identified, followed by the function with the lowest possible energy in the orthogonal space of the last one, and so on, up to the  $k$ th function with the minimum energy in the orthogonal subspace of the first  $k - 1$  functions.

$$u_i = \begin{cases} \arg \min_{f \in \mathbb{R}^p} E_G(f) \\ \text{such that } u_i \perp u_j, j < i, i \leq k \end{cases}$$

The following energy function states that if the variation in mean expression of any gene among the two populations is equivalent to the (signed) average of the difference between the mean expression for the genes that either activate or inhibit it, an expression shift will have limited power:

$$E_G(\delta) = \sum_{i: d_i^- \neq 0}^p \left( \delta_i - \frac{1}{d_i^-} \sum_{(j,i) \in \mathcal{E}} a_{ji} \delta_j \right)^2$$

The number of directed edges leading from any node to  $u_i$  is denoted by  $d_i^-$ .

Then, to achieve orthonormal functions with low intensity, the first few eigenvectors of  $M_G$  are employed to construct a lower dimension space.

Following that, a graph-structured two-sample test statistic is demonstrated. Hotelling's  $T^2$ -test, a classic location shift test, is a consistently most powerful invariant against global-shift alternatives for multivariate normal distributions. The statistical test  $T^2 = \frac{n_1 n_2}{n_1 + n_2} (\bar{x}_1 - \bar{x}_2)^T \hat{\Sigma}^{-1} (\bar{x}_1 - \bar{x}_2)$  is predicated on the sample mean shift's squared *Ma-halanobis norm*. In this work,  $T^2$ -statistics follow the nominal  $F$ -distribution, while Hotelling's test in the new area limited to its first  $k$  components is said to generate greater power than testing in the complete new space.

Subsequently, a systematic way for identifying nonhomogeneous subgraphs, or subgraphs of a large graph with a significant shift in means, is to examine each one individually. Due to the huge combinatorial issue posed by large sizes of graphs, it's critical to rapidly discover groups of subgraphs that all fit the null hypothesis of equal means. This is achieved by using a threshold on the value of the test statistic for every subgraph containing a particular network. The corresponding algorithm is described below.

**Figure 2.** Nonhomogeneous subgraph discovery algorithm

---

*Nonhomogeneous subgraph discovery algorithm*

---

**Input:**  $G, X_1, X_2, \alpha, q$

**Output:** selectedSubgraphs

1. selectedSubgraphs =  $\emptyset$ ;
  2. previousSubgraphs = nodes ( $G$ );
  3. prunedSubgraphs =  $\emptyset$ ;
  4. **for** each  $s \in \{1 \dots q-1\}$  **do**
  5.   checkedSubgraphs =  $\emptyset$ ;
  6.   **for** each previousSubgraph **do**
  7.     **for** each subgraph  $\in$  subgraphBoundary(previousSubgraph) **do**
  8.       **if** subgraph *has been checked or has a pruned subgraph* **then** next;
  9.       **if**  $s < q-1$  **then**
  10.          **if**  $upperBound(subgraph, G, X_1, X_2, q) < T_{\alpha, k}^2$  **then**
  11.            add subgraph to prunedSubgraphs;
  12.          **else**
-

---

```

13.      add subgraph to currentSubgraphs;
14.      end
15.      else
16.      for each q-subgraph  $\in$  subgraphBoundary(subgraph) do
17.      if q-subgraph has been checked or has a pruned subgraph
         then next
18.      else
19.      if  $\tilde{T}_k^2(q - subgraph, X_1, X_2) > T_{\alpha,k}^2$  then
20.      add q-subgraph to selectedSubgraphs
21.      end
22.      add q-subgraph to checkedSubgraphs
23.      end
24.      end
25.      end
26.      add subgraph to checkedSubgraphs
27.      end
28.      end
29.      set previousSubgraphs to currentSubgraphs
30. end

```

---

In the case of "limited" graphs over a certain level of connectivity and  $q$  large enough,  $v(g', q - s)$ , the  $(q - s)$ -neighborhood of  $g$ , increases at the initial stage of the above exact process, while the number of tests being conducted may not reduce significantly considering the number of feasible tests. As a result, a faster, approximation algorithm is introduced. The main idea is to find subgraphs with sample mean shifts in the first  $k$  components of a new space, where the Euclidean norm  $\|\hat{\delta}_{[k]}(g)\| = \|U_{[k]}^T(\underline{x}_1(g) - \underline{x}_2(g))\|$  is greater than a specified threshold. The output of substituting the *upper-Bound* with the following inequality in the Nonhomogeneous subgraph discovery algorithm produces an upper bound on  $\tilde{T}_k^2(g)$ .

$$\begin{aligned}
\|U_{[k]}^T(\bar{x}_1(g) - \bar{x}_2(g))\|^2 &\leq \|U^T(\bar{x}_1(g) - \bar{x}_2(g))\|^2 = \|\bar{x}_1(g) - \bar{x}_2(g)\|^2 \\
&\leq \|\bar{x}_1(g') - \bar{x}_2(g')\|^2 \\
&+ \max_{v_1, \dots, v_{q-s} \in v(g', q-s)} \|\bar{x}_1(u_1, \dots, u_{q-s} \in v(g', q-s)) \\
&- \bar{x}_2(u_1, \dots, u_{q-s} \in v(g', q-s))\|^2
\end{aligned}$$

This specifies a technique for detecting all subgraphs whose sample mean shift's Euclidean norm exceeds a certain threshold. Employing the  $T^2$ -test on these preselected subgraphs can also predict the group of subgraphs produced by the Nonhomogeneous subgraph discovery procedure.

A major issue with DE genes is the classification of non-significant differences as significant. The approaches presented by Lönnstedt and Speed (2002) can be used to solve such a problem.

Finally, the problem of multiple testing is raised due to the huge number of subgraphs assessed for homogeneity. This issue can be resolved by employing a permutation technique, which minimizes the amount of false positive subgraphs. Initially, the  $n_1 + n_2$  observations' class/population labels are permuted, and then the nonhomogeneous subgraph discovery process is implemented to the permuted data to give a specific amount of false positive subgraphs. This technique is repeated several times to provide an approximation of the distribution of Type I error rates.

The procedures' performance is first assessed on synthetic data, and subsequently on breast cancer microarray data examined using KEGG pathways.

## TEAK

Based on [18], Topology Enrichment Analysis framework (TEAK) was developed to discover active subpathways that underpin biological processes making use of the KEGG pathway database. Nodes represent gene products and/or complexes of gene products, while edges denote relationships between proteins or enzymes and are exploited to generate a set of unweighted adjacency matrices, which illustrate the KEGG pathways.

The subpathways extracted by the previous procedure can be either linear or nonlinear. Subpathways that consist of root to leaf linear paths are identified as linear. On the

contrary, nonlinear subpathways are distinguished by feed-forward loops that are adjacent and overlap.

To evaluate the linear and nonlinear subpathways, TEAK initially fits a context specific Gaussian Bayesian network for each subpathway using the Bayes Net Toolbox. A Gaussian Bayesian network is a Bayesian network that is a probabilistic graphical model, with all its nodes being linear Gaussians. Specifically, the Conditional Probability Distribution of  $Y$  for a continuous node  $Y$  with  $m$  continuous parents  $X_1, \dots, X_m$  is:

$$p(Y|x_1, \dots, x_m) = N(\beta_0 + \beta_1 x_1 + \dots + \beta_m x_m; \sigma^2)$$

Subsequently, for subpathways consisting of context specific data, TEAK uses the Bayesian Information Criterion (BIC) provided in the Bayes Net Toolbox and scores each Bayesian network.

$$Score_{BIC} = \log P(D|\hat{\theta}) - 0.5d \log N.$$

Finally, since BIC is capable of breaking, which means that each node's score is computed separately and then added together to get the final score, each sub-pathway's value is normalized by the amount of nodes in order to make the scores equivalent.

## **PATHiWAYS**

PATHiWAYS is another tool for pathway analysis. More specifically, it is a web server that can interpret the consequences of multiple changes in gene expression levels when it comes to signaling pathways. The approach, as detailed in [19], is explained below.

It is based on a probabilistic model of the pathway, in which the probabilities of signal transmission are calculated. Gene expression values represent the gene activity and, therefore, the presence or absence of a protein. The 90<sup>th</sup> percentile of the distribution of the probe activation probabilities is used in order to reduce the number of false positives caused by faulty probe observations.

After calculating the individual probability of each node, depending on the number of proteins they are composed of, a simple product of probabilities is computed to estimate the probability of signal transmission through the pathway.

Eventually, the final probabilities are compared and detect which stimulus–response circuits had their probabilities of signal transmission significantly altered.

## DEAP

DEAP, which is short for Differential Expression Analysis for Pathways, is a pathway analysis method for identifying relevant regulatory patterns from differential expression data that takes advantage of information about biological pathways. Unlike previous methods of analysis, DEAP takes advantage of existing knowledge about pathway structure and recognizes the path that is the most differentially expressed. This technique calculates the scores of each subpathway with the use of the DEAP algorithm, which is determined in [20].

Initially, to estimate the null distribution of the test statistics and compute the  $p$ -values, a random rotation technique was employed. Rotation testing asserts that pathway and set data come from independent random samples of a multivariate normal distribution with mean zero under the null hypothesis.

Subsequently, the DEAP algorithm is applied. The algorithm handles expression data that are composed using the following multivariate normal distribution:

$$E = d(\mu + g) + e ,$$

where  $d$  signifies if a gene is ‘on’ or ‘off’,  $\mu$  represents the ‘pathway effect’ and  $g$  and  $e$  are generated using a normal distribution with both means equal to 0 and variances  $\sigma^2_g$  and 1 respectively.

The procedure is based on the following discrete steps. At first, the expression data are overlaid onto the network and each path from the graph is separately examined. Afterward, a recursive function is implemented and estimates the minimum and maximum differential expression for each pathway considering the type of relationship between nodes by adding or subtracting all downstream nodes.

The preceding method is summarized by the following formulas:  $Score = \sum_{z \in reactants} E(z) + T(edge) * max_{recursive}$  and  $Score = \sum_{z \in reactants} E(z) + T(edge) * min_{recursive}$

The edge type is represented by  $T(edge)$  in the formula above and can either be 1 for activation or -1 for inhibition.

The path with the maximal absolute differential expression is detected by using and comparing the absolute value of the differential expression calculated for each pathway on the previous step.



Subsequently, the data were rotated  $n$  times to simulate a null distribution of the test statistic,  $s^*$ , and the DEAP score was recalculated for every rotation sample. The random rotation approach helps resolve difficulties, such as not directly comparable DEAP scores for different paths, due to variances in size and structure among pathways, and determines the statistical significance.

Finally, the  $p$ -value is determined as the proportion of simulated DEAP scores, whose value is greater than or equal to the observed DEAP score, divided by the number of scores that are at least as extreme as the observed DEAP score:

$$p = \frac{\#(s_i \geq s^*)}{n}$$

## GraphiteWeb

Another option is GraphiteWeb, which is an innovative web tool for network analyses and visualization for gene expression data from both microarray and RNA-seq studies. Given [21], it integrates topological and multivariate pathway studies with an efficient model of interactive network representations for simple comprehension of the results and uses a variety of multivariate gene set techniques. In addition, it uses multivariate gene set analysis including conventional hypergeometric enrichment, global test, GSEA, SPIA, and ClPPER, as well as the KEGG and Reactome pathway databases. In this paper, we will focus solely on the Enrichment Analysis (competitive and non-topological) approach.

Enrichment analysis uses the Fisher Exact test to estimate the odds of finding a certain number of genes in a specific pathway among the DEGs, denoted as  $n_{G,deg}$ . Within a set of  $N_{deg}$  genes, the likelihood  $P$  of seeing at least  $n_{G,deg}$  genes is calculated by

$$P(N_{G,deg} \geq n_{G,deg}) = \sum_{i=n_{G,deg}}^{N_{deg}} \frac{\binom{N_G}{i} \binom{N-N_G}{N_{deg}-i}}{\binom{N}{N_{deg}}},$$

where  $N$  is the actual population of genes tested,  $G$  denotes the pathway, and  $N_i$  and  $n_i$  measure the frequency of genes within every table cell.

Subsequently, using the Benjamini and Hochberg technique,  $P$ s are normalized.

The statistical methodology typically employed to identify DEGs in RNA-seq count data is built on the negative binomial distribution. Given the strong relationship be-

tween read count and gene length, the read count specifies the test's power in this scenario. The  $P$ -value correction for gene length is an option in graphite web for adjusting for this bias.

## PATHOME

PATHOME stands for Pathway and Transcriptome Information and is a computational approach for detecting differentially expressed subpathways. Its methodology from [22] is based on gene expression profiles of two control groups and relevant biochemical pathways.

At first, PATHOME divides the pathways into subpathways and then uses statistical tests to assess the significance of differential expression profiles alongside the pathway. The type of interaction is also considered.

The decomposition of the main pathway into linear paths is achieved using a depth-first search algorithm. Due to the huge number of possible paths resulting from the previous step, a selection step is used prior to the statistical significance test step to avoid such difficulties.

In order to select which segment of the subpathway will be statistically reviewed in the test step, the following rule is applied:

$$I^k = \arg \min_m \left\{ - \sum_{i=1}^m I(\text{sgn}(r_{i,i+1}^k \times e_{i,i+1}) = 1) + \sum_{i=1}^m R(\text{sgn}(r_{i,i+1}^k \times e_{i,i+1})) \right\} \\ + 1, m \in \{1, \dots, p-1\}, R(x) = \begin{cases} 0, & \text{if } x \in \{1\} \\ \infty, & \text{otherwise} \end{cases}$$

A subpathway is chosen and continuous to the test step if the association rule between the expression correlation and the edge information for the neighboring items along the path is agreed upon by both experimental groups, and both consecutive segments include at least four components.

The final step determines which subpathway has a statistically significant difference in correlation between two subsequent segments for the two studies. The significance is examined under the null hypothesis, in which the alternative hypothesis represents the case in which the global mean of the correlations between the two groups are different.

Finally, to determine significance, we employed the z-test statistic, considered multiple comparisons, and the FDR was set at 0.05.

## SubSPIA

The SPIA approach, mentioned above, was paired with a current subpathway analysis method to create the sub-SPIA method, which was used to find cancer-related pathways. [23] provides the exact technique. To avoid problems resulting from the k-clique structure, used to define subpathways in the original subpathway analysis, the sub-SPIA method uses the minimal-spanning-tree structure.

A minimal-spanning tree is a tree-like subgraph, in which all nodes are connected, without forming a cycle. Because of the sparse connections between genes and the indirect connectivity of DEGs, this technique outperforms the k-clique notion.

The implementation of sub-SPIA was done using the R programming language. The following steps outline the main idea behind this method. Initially, we reassemble the gene network based on the signaling pathway. Then, in the gene network that has been created, the DEGs are mapped, and, finally, the subpathways are identified and their statistical and perturbation significance is evaluated. The Kruskal algorithm is used to create the minimal-spanning tree and then remove any non-signature nodes remaining in the leaves of the MST.

To determine the statistical significance of each subpathway, the hypergeometric test and anomalous perturbation are employed. As in the SPIA tool, the present method contains two probabilities,  $P_{NDE}$  and  $P_{PERT}$ . The  $p$ -value can then be used to determine the pathway's enrichment significance using the following equation:

$$p = 1 - \sum_{x=0}^{r-1} \frac{\binom{t}{x} \binom{m-t}{n-x}}{\binom{m}{n}}$$

In the equation above,  $m$  represents the total number of genes in the genome, while  $t$  is the number of genes involved in the studied pathway. The variable  $t$  denotes the number of genes provided for study, of which  $r$  are participating in the same pathway.

The  $P_{PERT}$  is calculated the same way as shown in the SPIA method and is combined with  $P_{NDE}$  in order to form a new global probability,  $P_G$ .

## MinePath

Another tool for pathway analysis is MinePath, which combines knowledge from gene expression profiles and molecular pathways. MinePath recognizes functionally differential sub-paths among different phenotype classes. Focusing on [24], below is a basic outline of the methodology.

MinePath's general technique consists of five modular components that must be implemented. Initially, the gene expression data must be discretized so that the domain dimensionality is reduced. The supervised Entropy-based global discretization approach was implemented to convert gene expression values into binary equivalents that are either high (expressed) or low (non-expressed). In addition, because of the differences in the nomenclature of pathways and gene expression data, MinePath examines each gene's various probesets and indicates a combined expression value by employing a logic OR to the probeset values.

Then, following a depth-first search technique, each pathway is broken into all its sub-paths. The sub-paths that emerged are compared to the binary gene expression sample profiles provided as input. A collection of binary (Boolean) operations and a number of semantics that interpret the precise molecular nature of the underlying gene interactions are used to determine the functional capacity of a sub-path in a sample. MinePath handles two types of single gene regulatory relationships: activation/expression and inhibition, which are described by the AND and XOR Boolean operators, respectively. In the event of more complex sub-paths, MinePath uses an AND operator to merge the binary values of the path's final relation and the binary value of the sub-component path's investigated so far.

Subsequently, the most discriminant sub-paths are identified using a multi-parametric sub-path selection technique, which is implemented by the employment of feature selection and classification techniques. MinePath includes three independent filters to analyze the phenotype differential power of sub-paths and identify the most discriminant among them: coverage, p-value, and polarity, each with its own customizable threshold. Those sub-paths that pass all the filters are chosen and maintained as the most discriminant.

Finally, MinePath evaluates the relevance of the pathways and ranks them according to their  $p$ -value, which is calculated based on the following formula:

$$p - value_p = \frac{\left( \frac{(a_p - 1) + b_p}{a_p - 1} \right) \left( \frac{c_p + b_p}{c_p} \right)}{\left( \frac{n}{(a_p - 1) + c} \right)}$$

MinePath's final output is a  $p$ -value ranked list of pathways from which the user can choose one to visualize and study.

## HiPathia

HiPathia is a method that uses transcriptome data to calculate signal transduction along signaling pathways. [25] and [26] explain the technique.

To model the various cell functions in detail, each pathway is first broken down into circuits. The algorithm used by the HiPathia method models signal propagation by considering the level of activity of the proteins that make up the circuit. The simultaneous presence of the chain of proteins that connect the receptor to the effector, as well as the absence of inhibitor proteins that could compromise the signal's transduction along the circuit, in order to be active and thus transduce the signal to eventually trigger a function, is necessary for a circuit. The signal generated by the input node is communicated along the pathway as in the direction of the interactions and the output is collected by an output node, which activates a cell function. The signal is transmitted along the path according to the following recursive formula:

$$S_n = v_n \cdot \left( \prod_{S_a \in A} (1 - S_a) \right) \cdot \prod_{S_i \in I} (1 - S_i)$$

$S_n$  and  $v_n$  represent the signal intensity for the current node  $n$  and its normalized gene expression value respectively.  $A$  describes all the activation signals ( $S_a$ ) that are collected at the current node  $n$  from activation edges, and  $I$  describes the corresponding inhibitory signals ( $S_i$ ).

Finally, based on each circuit's structure, the last effector node will either detect variations in the nodes' activity or not.

**Table 1.** Pathway's scoring formula of Pathways Analysis tools

<i>Method</i>	<i>Date</i>	<i>Formula</i>
TAPPA	2007	$PCI = \sum_{i=1}^N \sum_{j=1}^N \text{sgn}(x_{is} + x_{js}) *  x_{is} ^{0.5} * \alpha_{ij} *  x_{js} ^{0.5}$
SPIA	2008	$P_G = c_i - c_i \cdot \ln(c_i), c_i = P_{NDE}(i) \cdot P_{PERT}(i)$
TopologyGSA	2010	$\Lambda = \frac{L_{H_0}(\hat{K}_1, \hat{K}_2)}{L_{H_1}(\hat{K}_1, \hat{K}_2)} = \frac{L_{H_0}(\hat{K})}{L_{H_1}(\hat{K})}$
PARADIGM	2010	$IPA(i) = \begin{cases} L(i, 1), & L(i, 1) > L(i, -1) \text{ and } L(i, 1) > L(i, 0) \\ -L(i, -1), & L(i, -1) > L(i, 1) \text{ and } L(i, -1) > L(i, 0) \\ 0, & \text{otherwise} \end{cases}$
GGEA	2011	$S := \sum_{t \in T_u} C(t), C(t) = \text{cons}(de_o, f_t(de_i))$
HotNet	2011	$h(g_j, g_k) = w(g_j, g_k) \times \{ S_j ,  S_k \}$
PRS	2012	$PRS(p_i) = \sum_{j=1}^{n_i} NS_j, NS = \begin{cases} NV * NW & \text{if } NV > 1 \\ 0 & \text{if } NV \leq 1 \end{cases}$
DEGraph	2012	$E_G(\delta) = \sum_{i: d_i^- \neq 0}^p \left( \delta_i - \frac{1}{d_i^-} \sum_{(j,i) \in \mathcal{E}} a_{ji} \delta_j \right)^2$
TEAK	2012	$Score_{BIC} = \log P(D \hat{\theta}) - 0.5d \log N$
PATHiWAYS	2013	Probabilistic model
DEAP	2013	$Score = \sum_{z \in \text{reactants}} E(z) + T(\text{edge}) * \max_{\text{recursive}} \text{ and } Score = \sum_{z \in \text{reactants}} E(z) + T(\text{edge}) * \min_{\text{recursive}}$
GraphiteWeb	2013	$P(N_{G,deg} \geq n_{G,deg}) = \sum_{i=n_{G,deg}}^{N_{deg}} \frac{\binom{N_G}{i} \binom{N - N_G}{N_{deg} - i}}{\binom{N}{N_{deg}}}$

PATHOME	2014	$I^k = \arg \min_m \left\{ - \sum_{i=1}^m I(\text{sgn}(r_{i,i+1}^k \times e_{i,i+1}) = 1) + \sum_{i=1}^m R(\text{sgn}(r_{i,i+1}^k \times e_{i,i+1})) \right\}$ $+ 1, m \in \{1, \dots, p-1\}, R(x) = \begin{cases} 0, & \text{if } x \in \{1\} \\ \infty, & \text{otherwise} \end{cases}$
SubSPIA	2015	$P_G = c_i - c_i \cdot \ln(c_i), c_i = P_{NDE}(i) \cdot P_{PERT}(i)$
MinePath	2015	Logical operators
HiPathia	2017	$S_n = v_n \cdot \left( \prod_{S_a \in A} (1 - S_a) \right) \cdot \prod_{S_i \in I} (1 - S_i)$

---

## Materials and Methods

### Datasets and processing

Two datasets are used in this study. The GSE2034 gene expression dataset was obtained from the Gene Expression Omnibus data repository available at <https://ncbi.nlm.nih.gov/geo/query/acc.cgi?acc=gse2034> and contains 286 breast cancer samples, of which 209 are ER-positive and 77 are ER-negative. The second dataset is a collection of 47 sub-paths in total from the KEGG database ([https://www.genome.jp/kegg-bin/show\\_organism?menu\\_type=pathway\\_maps&org=hsa](https://www.genome.jp/kegg-bin/show_organism?menu_type=pathway_maps&org=hsa)) of which 15 relate to cellular activities, 24 to signal propagation and 8 to cancer in general. The relation between two nodes is either activation or inhibition.

Due to the mapping of a gene to more than one Entrez identifiers, each Entrez identifier is translated to its associated gene. The expression value that results after the KEGG-IDs are combined into one gene is calculated as their average expression value. If a gene or gene ID involved in one of the investigated sub-paths does not match the dataset GSE2034, a new ‘noProbe’ gene is created with values equivalent to the mean of each corresponding sample.

The dataset of the sub-paths is handled in such a way that the nodes and edges for each sub-path can be distinguished and interpreted easier. More than one gene can be found in each node. In this case, the average value is assigned.

Moreover, the data from the two data sets is integrated to create new collective data structures. As a result, values such as expression values, p-values, and fold changes are directly linked to sub-path nodes, simplifying the analysis process.

### Computing the score

The methods implemented in the present paper are TAPPA, SPIA, PRS, TEAK, DEAP, GraphiteWeb, MinePath and HiPathia. The decision was made based on the degree of simplicity with which each method could be performed. The score of each sub-path was determined using the methodology described in each tool’s respective papers. Each approach offers details regarding the data normalization procedure, although the FDR correction method was employed for the DEAP and PRS tools. Due to their computational complexity, FDR correction was used in place of DEAP's random rotation approach and PRS' second normalization step's non-parametric permutation method.



Despite the fact that all techniques take pathway topology into consideration, we may generally identify two approaches to the problem. Tools TAPPA, GraphiteWeb, TEAK and PRS are based on probability theories and interpret pathway topology as the influence of nodes upon one another. Tools HiPathia, SPIA, DEAP and MinePath, on the other hand, focus on the relation type among genes and how it influences the output.

After computing the score of each sample for each unique sub-path according to the approach of the corresponding tool, a two-dimensional matrix emerged for every one of the tools, with rows representing samples and columns representing sub-paths.

### **Subpathway ranking**

After acquiring the scores of each sub-path for each tool independently, machine learning algorithms were used to train and evaluate the outcomes of each approach in order to perform the comparison among them.

Machine Learning is a subset of artificial intelligence that utilizes data and algorithms to model the learning process of a human while continually improving its accuracy [28]. Given that labeled data were available for this study and that the samples were to be divided into classes (ERpos, ERneg) based on the scores of the sub-paths, supervised learning techniques were considered. Thus, the Decision Trees algorithm was used to classify the findings and evaluate each approach since it also has the capability of recognizing the most important features; as a result, in addition to providing information about the accuracy of the results, it also provides insight into which sub-paths are significant.

The basis of the Decision Trees algorithm is the continuous division of the data by a given criterion. Two things -decision nodes and leaves- can explain the structure of the tree. The options or results are the leaves and the data is divided at the decision nodes [29].

Initially, since machine learning algorithms only comprehend numbers, the datasets representing the study's results of each approach were prepared and the samples' categorical classes were transformed into numerical variables.

Then, the modified datasets were divided, at a ratio of 70% to 30%, into training and testing sets. Each Machine Learning model was trained with the training sets that emerged from the previous step and evaluated using the corresponding testing sets. The

outcome is how accurate the models are for the data acquired from each approach and a list of the most significant sub-paths utilized as features for each approach's classification model predictions.

The scikit-learn package (<https://scikit-learn.org/stable/>) which offers pre-built machine learning functions for the Python programming language, was used to implement the aforementioned procedure.

## Results

### Predictive performance/ Data validation

The findings of each methodology employed in this study are provided in this section and are presented in [Table 2](#).

Accuracy, which is the proportion of correctly predicted data points among all the data points [30], is the parameter used to assess the performance of each approach. The tool or tools with the highest accuracy are highlighted. Overall, the accuracy of every technique is at least satisfactory, and for tools with an accuracy rate greater than 75%, it can be described as very good.

It is important to note that, when the findings were corrected using the Benjamini and Hochberg approach in the case of GraphiteWeb, the classification model's accuracy declined. One interpretation of such a reduction is improved capacity for adaption to new, previously unobserved data.

**Table 2.** Predictive performance of each tool

<i>Tool</i>	<i>Accuracy</i>
TAPPA	65,12%
PRS	83,72%
TEAK	67,44%
DEAP	82,56%
GraphiteWeb	75,58%
MinePath	68,6%
HiPathia	<b>84,88%</b>

However, despite the relatively good accuracy results, no common sub-paths could be identified across the tools in terms of the feature importance of each methodology. Consequently, no further information could be derived about the pathways because our study was unable to provide us with the most discriminant sub-paths.

## Tools comparison

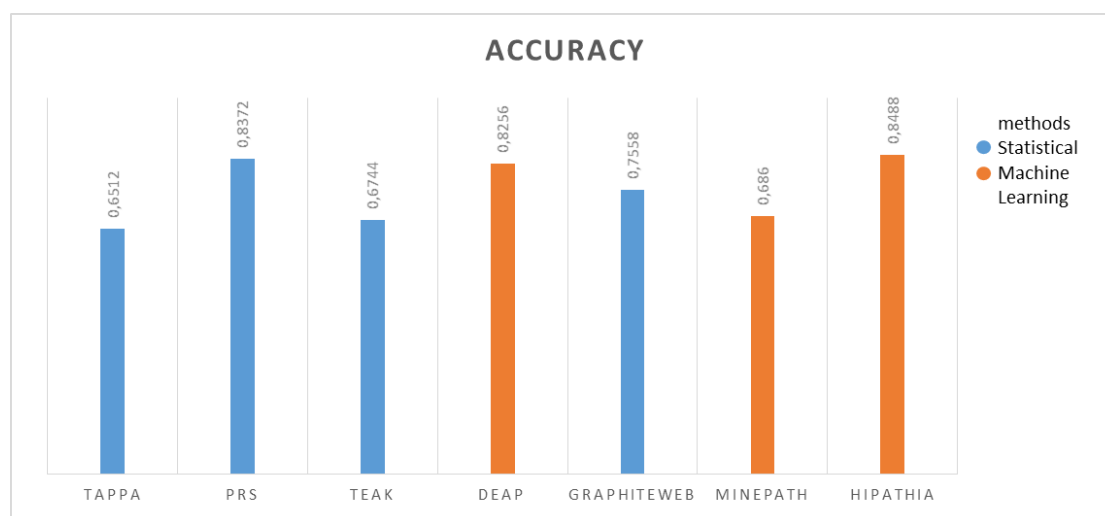
This study's primary goal was to compare several pathway activity analysis tools that use statistical and machine learning techniques. The comparison considers both each method individually and the two fundamental approaches collectively (see Section [“Computing the score”](#)).

Primarily, as demonstrated in [Table 2](#), HiPathia has the best predictive performance with a value of 84,88%, while the worst performance was TAPPA's with 65,12% accuracy. The performance of the remaining tools range from 65% to 84% and exceeds 75% for more than half of them.

Overall, the tools with accuracy greater than 80% are PRS, DEAP and HiPathia; PRS is based on statistical methods, while DEAP and HiPathia are predicated on Machine Learning algorithms. It is obvious that, in this study, tools based on Machine Learning algorithms outperform those based on statistical methods on average, when the main approach of each method is taken into account.

Additionally, there are variations when it comes to the types of values that each tool's scoring technique handles. While some methods employ non-binary data, others use binary values for gene expression. Given this, it is clear that techniques that utilize continuous values are preferred over those that use discrete valued data. This is due to the possibility that, even though categorizing genes as active or inactive is more practical and effective, important information may be missed.

**Figure 3.** Predictive Performance of each tool based on the method



However, the tools used in this paper are not sufficient to demonstrate that Machine Learning techniques are superior to Statistics, because there are only 7 tools in total and their distribution between the two main approaches is not proportional, which is extremely likely to influence the results. In addition, it cannot help with sub-pathway targeting for medical treatment, since no significant sub-pathways were discovered.

## Discussion

In this work, we implemented the scoring techniques for a number of Pathway Analysis tools that either rely on Machine Learning algorithms or statistical methods to identify similarities and differences among them. The findings of this research support the preference of Machine Learning over statistical methods, as well as the usage of non-binary gene expression data, but given the limitations observed the conclusions should be regarded cautiously.

Machine Learning is widely used in the field of Pathway Analysis due to the continuously growing amount of information in biology and the capability of Machine Learning algorithms to manage vast and complicated datasets [31]. Additionally, given that personalized therapies are the future of medicine, Machine Learning provides the tools needed to accomplish this purpose, because of its capacity to comprehend biological processes [32]. All of this, along with the exponential increase in computing power that is now available, has allowed Machine Learning to be considered as a promising technology for Pathway Analysis [33]. However, the application of Machine Learning in healthcare has some drawbacks that must be resolved, such as poor data quality and ethical dilemmas [34].

Multiple studies have been conducted to determine the type of gene expression data—binary and non-binary—that yields the most beneficial outcomes, while it should be mentioned that the majority of the methods examined in this study dealt with continuous data. Genomic data cannot simply be classified as on or off, because they are continuous, therefore they must be translated into discrete values. By translating the data it is likely to result in the loss of potentially important information, which is a very significant drawback [36], regardless of the fact that binary data require less processing time. As a result, current research attempts to combine them in an effort to optimize their benefits and minimize their disadvantages. Therefore, as we also discovered from the literature review, there is a preference for non-binary valued gene expression data, or at least a tendency of transitioning from binary to continuous values.

The abundance of genomic platforms available is a major issue that has been identified in numerous bioinformatics studies, while several studies have been conducted with the goal of comparing and determining the best platform or attempting to merge different databases [40]. Given that most datasets are obtained using various genomic platforms

and processing techniques [41], it is highly likely that this limitation contributed to this study's inability to discover common significant sub-paths between two or more tools. This is due to variations in the platform design, synthesis and probe annotation [42], which lead to different outcomes.

Other scientific studies and experiments can be conducted taking into account both the positive and negative findings of this research. One approach could be applying additional tools in this study's scripts to ensure that the findings are unbiased and, given the availability of databases, using datasets from various genomic platforms to overcome the problem of correlating genes across multiple databases and thus the inability of identifying common significant sub-paths. Another approach could be concentrating on non-binary gene expression data and employing mostly Machine Learning to analyze gene expression and gene regulatory networks in future works. As a consequence, by utilizing the capabilities of Machine Learning technology and enhancing existing pathway analysis techniques, the rates of accurate medical diagnoses could increase.

## Conclusions

Pathway analysis is a promising technique for more precise medical diagnosis and determining the genetic basis of disorders. It makes use of current knowledge to better comprehend biological processes by combining both gene expression data and gene topology. However, a number of pathway analysis tools have been developed, each of which employs its own algorithm for pathway scoring that is either based on statistical techniques or machine learning algorithms. These scoring methodologies constituted the subject of this comparison study.

Overall, the outcomes indicate that Machine Learning-based methodologies perform better than those based on statistical methods. When looking at each tool separately (see [Table 2](#)), HiPathia had the highest accuracy rate, while TAPPA performed the worst. Furthermore, a significant proportion of the tools analyzed handle non-binary gene expression values, indicating their preference over binary data. Unfortunately, the research only analyzed a limited number of tools, and no significant common sub-paths between the tools were found, making it difficult to confidently accept the findings.

Based on the results, we can recommend Machine Learning algorithms as a better technique for pathway analysis, but it would be preferable to conduct a new study that incorporates proportionately additional tools from both approaches as well as apply this paper's scripts to gene expression data from several genomic platforms. Also, choosing continuous data over discrete values is suggested. As a result, we will be able to identify the optimal method for future studies with greater confidence.

It is important to utilize every knowledge and technology provided to us, so that better and more accurate results are obtained every time. Consequently, as we get better at making sense of the data that is already available, more precise technologies will become available. These technologies will offer more precise medical diagnoses and, possibly, cures for diseases that we still don't fully understand.



## References

- [1] Miguel A. García-Campos, Jesús Espinal-Enríquez, and Enrique Hernández-Lemus, “Pathway Analysis: State of the Art,” *Front. Physiol.*, Dec. 2015.
- [2] Tuan-Minh Nguyen, Adib Shafi, Tin Nguyen, and Sorin Draghici, “Identifying significantly impacted pathways: a comprehensive review and assessment,” *Genome Biol.*, Oct. 2019.
- [3] “KEGG,” *Wikipedia*. Feb. 11, 2022. [Online]. Available: <https://el.wikipedia.org/wiki/KEGG>
- [4] “KEGG PATHWAY Database,” *KEGG: Kyoto Encyclopedia of Genes and Genomes*. Mar. 24, 2022. [Online]. Available: <https://www.genome.jp/kegg/pathway.html>
- [5] “BioCarta Pathways,” *SciCrunch / Research Resource Resolver*. [https://scicrunch.org/ADC/resolver/RRID:SCR\\_006917](https://scicrunch.org/ADC/resolver/RRID:SCR_006917)
- [6] “Home - Reactome Pathway Database,” *Reactome*. <https://reactome.org/>
- [7] Ivana Ihnatova, Vlad Popovici, and Eva Budinska, “A critical comparison of topology-based pathway analysis methods,” *PLOS ONE*, Jan. 2018.
- [8] Shouguo Gao and Xujing Wang, “TAPPA: topological analysis of pathway phenotype association,” *Oxf. Acad.*, Sep. 2007.
- [9] Adi Laurentiu Tarca *et al.*, “A novel signaling pathway impact analysis,” *Natl. Cent. Biotechnol. Inf.*, Jan. 2009.
- [10] Maria Sofia Massa, Monica Chiogna, and Chiara Romualdi, “Gene set analysis exploiting the topology of a pathway,” *BMC*, Sep. 2010.
- [11] Charles J Vaske *et al.*, “Inference of patient-specific pathway activities from multi-dimensional cancer genomics data using PARADIGM,” *Natl. Cent. Biotechnol. Inf.*, Jun. 2010.
- [12] Ludwig Geistlinger, Gergely Csaba, Robert Küffner, Nicola Mulder, and Ralf Zimmer, “From sets to graphs: towards a realistic enrichment analysis of transcriptomic systems,” *Natl. Cent. Biotechnol. Inf.*, Jul. 2011.
- [13] “HotNet,” *Raphael Lab*. <http://compbio.cs.brown.edu/projects/hotnet/>

- [14] Fabio Vandin, Eli Upfal, and Benjamin J Raphael, “Algorithms for detecting significantly mutated pathways in cancer,” *Natl. Cent. Biotechnol. Inf.*, Mar. 2011.
- [15] Maysson Al-Haj Ibrahim, Sabah Jassim, Michael Anthony Cawthorne, and Kenneth Langlands, “A Topology-Based Score for Pathway Enrichment,” *Natl. Cent. Biotechnol. Inf.*, Mar. 2012.
- [16] Laurent Jacob, Pierre Neuvial, and Sandrine Dudoit, “DEGraph: differential expression testing for gene networks,” *Bioconductor*, Oct. 2014.
- [17] Laurent Jacob, Pierre Neuvial, and Sandrine Dudoit, “More Power via Graph-Structured Tests for Differential Expression of Gene Networks,” *Proj. Euclid*, Jun. 2012.
- [18] Thair Judeh, Cole Johnson, Anuj Kumar, and Dongxiao Zhu, “TEAK: Topology Enrichment Analysis framework for detecting activated biological subpathways,” *Natl. Cent. Biotechnol. Inf.*, Feb. 2013.
- [19] Patricia Sebastián-León, José Carbonell, Francisco Salavert, Rubén Sanchez, Ignacio Medina, and Joaquín Dopazo, “Inferring the functional effect of gene expression changes in signaling pathways,” *Oxf. Acad.*, Jun. 2013.
- [20] Winston A. Haynes, Roger Higdon, Larissa Stanberry, Dwayne Collins, and Eugene Kolker, “Differential Expression Analysis for Pathways,” *Natl. Cent. Biotechnol. Inf.*, Mar. 2013.
- [21] Gabriele Sales, Enrica Calura, Paolo Martini, and Chiara Romualdi, “Graphite Web: web tool for gene set analysis exploiting pathway topology,” *Natl. Cent. Biotechnol. Inf.*, May 2013.
- [22] S Nam *et al.*, “PATHOME: an algorithm for accurately detecting differentially expressed subpathways,” *Natl. Cent. Biotechnol. Inf.*, Oct. 2014.
- [23] Xianbin Li, Liangzhong Shen, Xuequn Shang, and Wenbin Liu, “Subpathway Analysis based on Signaling-Pathway Impact Analysis of Signaling Pathway,” *PLOS ONE*, Jul. 2015.
- [24] Lefteris Koumakis *et al.*, “MinePath: Mining for Phenotype Differential Subpaths in Molecular Pathways,” *Natl. Cent. Biotechnol. Inf.*, Nov. 2016.

- [25] Kinza Rian *et al.*, “Genome-scale mechanistic modeling of signaling pathways made easy: A bioconductor/cytoscape/web server framework for the analysis of omic data,” *ScienceDirect*, May 2021.
- [26] Marta R Hidalgo, Cankut Cubuk, Alicia Amadoz, Francisco Salavert, José Carbonell-Caballero, and Joaquin Dopazo, “High throughput estimation of functional cell activities reveals disease mechanisms and predicts relevant clinical outcomes,” *Natl. Cent. Biotechnol. Inf.*, Jan. 2017.
- [27] Lefteris Koumakis, “Computational methods for knowledge discovery from heterogeneous data sources: methodology and implementation on biological and molecular sources,” Technical University of Crete, School of Production Engineering and Management, 2014.
- [28] IBM Cloud Education, “Machine Learning,” *IBM*, Jul. 15, 2020.  
<https://www.ibm.com/cloud/learn/machine-learning>
- [29] “Decision Trees for Classification: A Machine Learning Algorithm,” *Xoriant*.  
<https://www.xoriant.com/blog/decision-trees-for-classification-a-machine-learning-algorithm>
- [30] “Accuracy (error rate),” *DeepAI*. <https://deepai.org/machine-learning-glossary-and-terms/accuracy-error-rate>
- [31] Hayat Ali Shah, Juan Liu, Zhihui Yang, and Jing Feng, “Review of Machine Learning Methods for the Prediction and Reconstruction of Metabolic Pathways,” Jun. 2021.
- [32] Kexin Huang, Cao Xiao, Lucas M. Glass, Cathy W. Critchlow, Greg Gibson, and Jimeng Sun, “Machine learning applications for therapeutic tasks with genomic data,” vol. 2, no. 10, Oct. 2021.
- [33] Miroslava Cuperlovic-Culf, “Machine Learning Methods for Analysis of Metabolic Data and Metabolic Pathway Modeling,” Jan. 2018.
- [34] Junjie Peng, Elizabeth C. Jury, Pierre Dönnès, and Coziana Ciurtin, “Machine Learning Techniques for Personalised Medicine Approaches in Immune-Mediated Chronic Inflammatory Diseases: Applications and Challenges,” Sep. 2021.

- [35] Marzyeh Ghassemi, Tristan Naumann, Peter Schulam, Andrew L. Beam, Irene Y. Chen, and Rajesh Ranganath, “A Review of Challenges and Opportunities in Machine Learning for Health,” May 2020.
- [36] Koji Kyoda, Mineo Morohashi, Shuichi Onami, and Hiroaki Kitano, “A gene network inference method from continuous-value gene expression data of wild-type and mutants,” Feb. 2000.
- [37] Andrew McDavid *et al.*, “Data exploration, quality control and testing in single-cell qPCR-based gene expression experiments,” Feb. 2013.
- [38] Yoram Ben-Shaul, Hagai Bergman, and Hermona Soreq, “Identifying subtle interrelated changes in functional gene categories using continuous measures of gene expression,” Jan. 2005.
- [39] Lorena Postiglione, Marco Santorelli, Barbara Tumaini, and Diego di Bernardo, “From a discrete to continuous actuation for improved real-time control of gene expression in mammalian cells,” 2016.
- [40] Jason Rudy and Faramarz Valafar, “Empirical comparison of cross-platform normalization methods for gene expression data,” Dec. 2011.
- [41] Andrey A. Shabalin, Hakon Tjelmeland, Cheng Fan, Charles M. Perou, and Andrew B. Nobel, “Merging two gene-expression studies via cross-platform normalization,” 2008.
- [42] Anna V. Tinker, Alex Boussioutas, and David D.L. Bowtell, “The challenges of gene expression microarrays for the study of human cancer,” *ScienceDirect*, vol. 9, no. 5, May 2006.
- [43] Tracy Tucker *et al.*, “Comparison of genome-wide array genomic hybridization platforms for the detection of copy number variants in idiopathic mental retardation”.